Journal of Magnetic Resonance **136,** 118–126 (1999)
Article ID jmre.1998.1590, available online at http://www.idealibrary.com on IDEAL®

A Method for Determining B_1 Field Inhomogeneity. Are the Biases Assumed in Heteronuclear Relaxation Experiments Usually Underestimated?

Marc Guenneugues,*[,1] Patrick Berthault,† and Hervé Desvaux†[,2]

*Département d'Ingéniérie des Protéines, and †Service de Chimie Moléculaire, Laboratoire Commun de R.M.N., C.E.A./Saclay, F-91191 Gif sur Yvette, France

E-mail: hdesvaux@cea.fr

Received May 1, 1998

We describe a method allowing the determination of the effective B_1 field amplitude distribution in a high-resolution NMR spectrometer. This method which can be adapted to almost any sequence, essentially consists of a nutation followed by a purging B_0 gradient pulse. Experimental results obtained with this approach are described in homonuclear and heteronuclear cases. The experimental distributions are used to estimate the biases induced by B_1 inhomogeneity, as well as the loss of RF power on heteronuclear transverse self-relaxation rate determination. In this type of measurement, the experimental biases induced on the intensities can be as large as 5% for long mixing times.

Key Words: **RF field homogeneity; heteronuclear relaxation.**

I. INTRODUCTION

The classical NMR method to explore protein dynamics consists of measuring the longitudinal and transverse self-relaxation rates and the heteronuclear dipolar cross-relaxation rates (nOe) (*1–4*). It has recently been shown that promising information on protein structure or dynamics, such as determination of the anisotropic Brownian reorientation (*5–7*) or localization and characterization of fast chemical exchange processes (*8*), can be deduced from precise measurements of the self-relaxation rates usually followed by statistical treatment. The uncertainties of the determined relaxation rates are usually derived by considering the errors in the measured intensities of dual experiments and are found to be on the order of 1%. However it was statistically shown that this leads to an underestimation of the uncertainty by a factor of 4 (*9*). This discrepancy may, at least in part, arise from hardware imperfections that can introduce systematic biases not detected in reproduced experiments. To avoid biases resulting from the CPMG approach (*10*), one generally rather measures the heteronucleus spin–lattice relaxation rate in the presence of an RF field ($R_{1\rho}$). Interpretation of the obtained rates requires the knowledge of the RF field strength in order to correct for the offset effects and to evaluate the presence of fast chemical exchange contributions to the relaxation. In the present paper, we report a reliable experimental procedure for determining quickly and precisely the effective RF field strength experienced by the sample, as well as its inhomogeneity. Effects of the latter on the measured intensities in a typical $R_{1\rho}$ experiment are then further explored.

II. B_1 FIELD INHOMOGENEITY IN AMPLITUDE AND PHASE

Two different schemes can be considered for determining the RF field inhomogeneity, either building a pictorial 3D map giving the RF field amplitude and direction in each voxel (*11, 12*) or measuring the distribution of the RF field, i.e., the fraction of the sample which experiences a given RF field strength (*13–16*). The first scheme is obviously more detailed but actually difficult to exploit, because it requires the use of the reciprocity theorem (*17*). Indeed one measures a magnetization summed over the sample volume so that the interesting information does not lie in the spatial distribution but in the distribution all over the sample of the amplitude and/or phase of an applied RF field. This is what gives the second scheme based on a simple nutation experiment (*13*).

We consider a spin $\frac{1}{2}$, I, noncoupled to any other spin, and an inhomogeneous RF field at the Larmor frequency of spin I. We neglect B_0 inhomogeneity, since resolution as high as 0.1 Hz is now classical on commercial spectrometers. We consider a voxel with an associated magnetization $I(v) = I_0\, dv$. In this voxel, the RF field amplitude is $2\omega_1(v)$ while its phase in the rotating frame relative to the Ox axis is $\phi(v)$. After application of an on-resonance irradiation of duration t_1 long relative to the transient phenomena, the components

[1] Present address: Bijvoet Center for Biomolecular Research, Utrecht University, Padualaan 8, 3584 CH Utrecht, The Netherlands.

[2] To whom correspondence should be addressed.

1090-7807/99 $30.00

of a magnetization initially aligned along the Oz axis become in the frame rotating at the irradiation frequency ω_I

$$I_x(v) = I_0 \sin(\omega_1(v)t_1)\sin\,\phi(v)dv \quad [1a]$$

$$I_y(v) = -I_0 \sin(\omega_1(v)t_1)\cos\,\phi(v)dv \quad [1b]$$

$$I_z(v) = I_0 \cos(\omega_1(v)t_1)dv. \quad [1c]$$

The components of the total magnetization are obtained by integration on the sample volume $\mathcal{V}$:

$$I_x = I_0 \int_{\mathcal{V}} \sin(\omega_1(v)t_1)\sin\,\phi(v)dv \quad [2a]$$

$$I_y = -I_0 \int_{\mathcal{V}} \sin(\omega_1(v)t_1)\cos\,\phi(v)dv \quad [2b]$$

$$I_z = I_0 \int_{\mathcal{V}} \cos(\omega_1(v)t_1)dv. \quad [2c]$$

We can now replace the sum on the volume by an integral on the proportion of the voxels that experience an RF field of amplitude ω_1 and of phase ϕ. We respectively denote $\mathcal{P}(\omega_1)d\omega_1$ as the fraction of the sample experiencing an RF field amplitude in the range $[\omega_1;\ \omega_1 + d\omega_1]$ and $\mathcal{P}(\phi;\ \omega_1)d\phi$ as the fraction of the sample experiencing an RF field of amplitude ω_1 and of phase in the range $[\phi;\ \phi + d\phi]$. Equations [2] may then be rewritten as

$$I_x = I_0 \int_0^\infty \left[\int_0^{2\pi} \mathcal{P}(\phi;\ \omega_1)\sin\,\phi d\phi\right]\mathcal{P}(\omega_1)\sin(\omega_1 t_1)d\omega_1 \quad [3a]$$

$$I_y = -I_0 \int_0^\infty \left[\int_0^{2\pi} \mathcal{P}(\phi;\ \omega_1)\cos\,\phi d\phi\right]\mathcal{P}(\omega_1)\sin(\omega_1 t_1)d\omega_1 \quad [3b]$$

$$I_z = I_0 \int_0^\infty \mathcal{P}(\omega_1)\cos(\omega_1 t_1)d\omega_1. \quad [3c]$$

• Recording the transverse magnetization following the irradiation gives a signal proportional to $I_x - iI_y$, that is,

$$-iI_0\left(\int_0^\infty \left[\int_0^{2\pi} \mathcal{P}(\phi;\ \omega_1)e^{i\phi}d\phi\right]\mathcal{P}(\omega_1)\sin(\omega_1 t_1)d\omega_1\right)e^{-i\omega_2 t_2}. \quad [4]$$

Fourier transformation along t_2 makes it possible discriminate the studied nuclei according to their resonance frequency (ω_2). The condition of on-resonance RF irradiation leads us to consider the spin such that $\omega_2 = \omega_I$. The free-induction decay obtained can be further analyzed by real Fourier transformation giving a dispersive spectrum that characterizes the RF field experienced by the different nuclei during the irradiation. Using a Hilbert transformation (which is blindly done by adjusting the zero-order phase correction to 90°), one ends up with an absorptive spectrum along the indirect dimension, the intensity at each frequency being proportional to $\mathcal{P}(\omega_1)[\int_0^{2\pi} \mathcal{P}(\phi;\ \omega_1)e^{i\phi}d\phi]$, according to Eq. [4]. It thus depends on the amplitude and phase distribution of the RF field during the irradiation. The expected shape of the spectrum is thus a Dirac function for a perfectly homogeneous RF field. Actually, the design of the coil induces restraints on the RF field amplitude, and therefore the resulting spectrum is asymmetrical. Phase inhomogeneities at a given field strength will lower the observed intensity at this frequency. The effects on the observed spectrum are thus hard to predict but should not restore the symmetry lost by amplitude distribution.

• We consider now the case where a purging gradient pulse has been applied to destroy any transverse magnetization. When applying a read pulse of duration $T_{90°}$, the observed signal becomes

$$I_0\left(\int_0^\infty \mathcal{P}(\omega_1)\cos(\omega_1 t_1)d\omega_1\right)F_{\mathrm{rp}}e^{-i\omega_2 t_2}, \quad [5]$$

where

$$F_{\mathrm{rp}} = -i\int_0^\infty \left[\int_0^{2\pi} \mathcal{P}(\phi;\ \omega_1)e^{i\phi}d\phi\right]\mathcal{P}(\omega_1)\sin(\omega_1 T_{90°})d\omega_1 \quad [6]$$

is a multiplicative constant resulting from assuming that it is independent of the irradiation pulse. This assumption will be discussed below. As above, Fourier transformation along t_2 allows the discrimination of the studied nuclei, while a real Fourier transformation of the resulting interferogram directly leads to an absorptive spectrum in which the intensity is proportional to $\mathcal{P}(\omega_1)$ (Eq. [5]), which is only a function of the amplitude distribution of the applied RF field.

The inhomogeneity which should be considered depends on the sequence. In the case of a simple spin-lock pulse, the relative phase of the RF field over the sample influences the final observed intensities through a weighted average (Eqs. [3a] and [3b]). In contrast, taking advantage of the axial symmetry around Oz by projecting (or rotating) the magnetization from this axis to the effective field and back again at the end of the spin-lock allows one to disregard the effect of the phase distribution and to restrict the dependence of the magnetization evolution to the RF field strength only.

In the above calculation, we have assumed that the RF field $\omega_1(v)$ is time independent in frequency, amplitude, and phase. It can however be extended to the time-dependent case by integrating the Liouville–von Neumann equation. Although Eqs. [1] must be replaced by more complex expressions, the final results (Eqs. [3]–[5]) are the same except that $\mathcal{P}(\omega_1)d\omega_1$ represents a convolution of the fraction of the sample experiencing a given RF field by the probability of finding it. None of the experiments we have run have proved that this more complex treatment gives a closer description of the reality.

The extension of the derivation to the case where the RF field is not applied on-resonance is straightforward. The magnetization vectors process then along an effective field axis which is tilted by an angle θ from the static magnetic field direction

$$\tan\theta = \frac{\omega_1}{\Delta}, \qquad [7]$$

where Δ is the frequency offset. Following the evolution of the transverse magnetization does not lead to a direct determination of the RF field distribution, while the evolution of the longitudinal magnetization still gives access to the inhomogeneity in amplitude of the effective field Ω, where

$$\Omega = \sqrt{\omega_1^2 + \Delta^2}. \qquad [8]$$

This solution can then be used to determine precisely the RF field strength for an irradiation out of resonance, a useful issue which takes into account the variation of the Q value of the coil with the irradiation frequency.

One should also take into account the magnetization decay due to relaxation occurring during the irradiation ($\exp(-R_{2\rho}^{\text{off.}}t_1)$). However, this relaxation rate $R_{2\rho}^{\text{off.}} = \frac{1}{2}(\sin^2\theta R_1 + (1 + \cos^2\theta)R_2)$ is on the order of the longitudinal R_1 and transverse R_2 relaxation rates of the studied nuclei, that is, hertzs or tens of hertz. As will be shown below, the magnetization decay due to RF field inhomogeneity is faster by at least one order of magnitude, enabling us to neglect this contribution in the following.

The generalization to a real spin system of the calculation performed on an isolated spin $\frac{1}{2}$ reveals that (i) the dipolar cross-relaxation between the spins is almost never secular, since due to the difference of their offsets, their difference of precession frequencies is much larger than the cross-relaxation rates; and (ii) the J coupling Hamiltonian can be neglected as soon as the RF field strength ω_1 is much larger than the J value. A consequence of this resides in the need of proton decoupling when the RF field distribution on a X nucleus is studied.

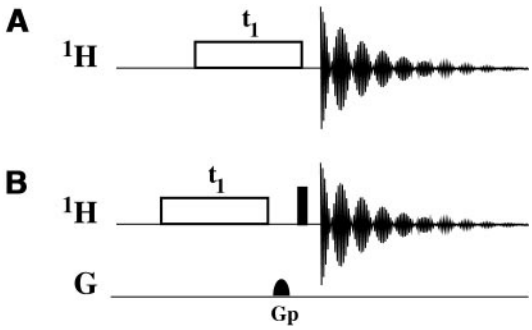

FIG. 1. Pulse schemes used to determine the RF field homogeneity. (A) gives the RF field inhomogeneity in amplitude and phase while (B) gives the RF field inhomogeneity in amplitude only. The open box corresponds to the nutation period of duration t_1. The narrow filled box is a 90° pulse that can be applied at high power or at the power used in the nutation period. Gp is a purging gradient pulse. t_1 is incremented by a value of $1/(2 * \nu_{\max})$, according to the Nyquist criterion, when one wants to study the response of the irradiation in the range [0: $\nu_{\max}$]. Further data processing are described in the text. For sequence (B), if the distribution of effective field amplitude Ω is desired, the nutation can be applied off-resonance. The offset Δ is then the distance between the RF frequency and the Larmor frequency of the studied spin defined by the chosen column.

III. MEASUREMENT OF B_1 INHOMOGENEITY

A. Homonuclear Case

Figure 1 shows two sequences used to measure the RF field inhomogeneity. The sequence of Fig. 1A was suggested by Bax (*15*) and is designed to measure the RF field inhomogeneity arising from amplitude and phase variations all over the sample. It can only be used when RF irradiation is applied exactly on-resonance. The sequence of Fig. 1B allows determination of the RF field inhomogeneity in amplitude. It essentially consists of a nutation experiment followed by a purging gradient pulse to keep only the z component of the magnetization and finally a read pulse, here, a simple 90° hard pulse. Figure 2A shows an example of the RF inhomogeneity measured on-resonance at a given RF field strength observed via the sequences of Figs. 1A and 1B on a broadband inverse probehead. It can be observed that the RF field inhomogeneity is rather small (about 4.4% at half-width). The curves exhibit an asymmetrical shape as expected. The highest probability field strength is found to be the same in both cases. However this probability is higher for the RF field amplitude distribution spectrum than for the amplitude and phase distribution spectrum. Moreover the full-width at middle-height (FWMH) is larger when considering the complete inhomogeneity than that for the amplitude inhomogeneity (310 versus 280 Hz).

According to Eqs. [4] and [5], the ratio between these two spectra gives the phase inhomogeneity at each field strength, if one neglects the multiplicative constant. This ratio (Fig. 2B) is not constant with ω_1, meaning that the phase and

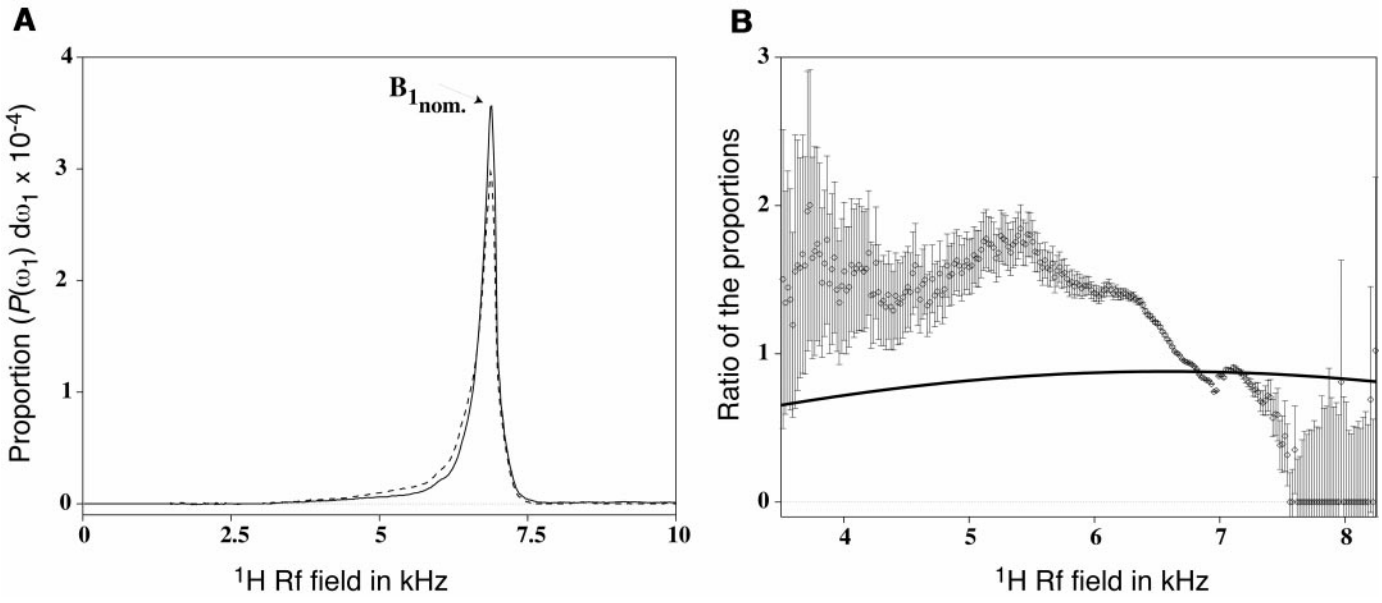

FIG. 2. (A) Distribution of ^{1}H RF field observed on a Bruker *z* gradient broadband inverse probehead equipping a Bruker DRX500 spectrometer. The sample is a 10 mM solution of α cyclodextrin in D_2O at 298 K. Displayed are traces along F_1 at the frequency of the H1 proton extracted from the 2D spectrum obtained according to the procedure described in the text. The carrier frequency was fixed to this proton Larmor frequency. The solid line corresponds to the distribution in amplitude obtained by the sequence of Fig. 1B, while the dotted line has been obtained by the sequence of Fig. 1A. For this particular spectrum the RF field strength of the 90° hard pulse of the sequence of Fig. 1B is the same as that used during the nutation. The γB_1 field value measured by a 360° pulse is 6.6 kHz while $\gamma B_{1\,\mathrm{nom.}}$, the RF field for which the probability is maximum, is larger: 6.89 kHz (*16*). (B) Ratio of the two previous distributions. The error bars derive from estimation of the noise calculated from the fluctuation of the B_1 field in the wings of the distribution. The solid line superimposed corresponds to the function $\sin(\omega_1 T_{90^\circ})$. A clear discrepancy between the curve and the data points is observed, showing that the RF field inhomogeneity depends on the sequence. The spectral width in the F_1 dimension is 10 kHz, the 2D spectrum is composed of 400 FIDs, while the processed spectrum contains 512 real points in the F_1 dimension. The spectrum corresponds to the column for the on-resonance peak. No apodization function was applied along F_1.

amplitude are not fully independent. This statement relies on the assumption that the irradiation and read pulses are independent. If we assume now that in each voxel the phase and amplitude homogeneities are constant during the pulse sequence, then after a read pulse applied on-resonance and at the same power level as the irradiation pulse, the recorded signal becomes

$$-iI_0\left[\int_0^{\infty}\mathcal{P}'(\omega_1)\cos(\omega_1 t_1)\int_0^{2\pi}\mathcal{P}(\phi;\,\omega_1)e^{i\phi}d\phi\right]\cdot e^{-i\omega_2 t_2} \qquad [9]$$

with $\mathcal{P}'(\omega_1) = \mathcal{P}(\omega_1)\sin(\omega_1 T_{90^\circ})$. The final spectrum is thus the same as that obtained by sequence 1A except that the measured probabilities are multiplied by $\sin(\omega_1 T_{90^\circ})$. The sequence of Fig. 2B is then no longer suited for determination of the RF field amplitude distribution, since it also contains the phase inhomogeneity information. Figure 2B shows that the ratio between the probabilities found using sequences 1A and 1B is not proportional to $\sin(\omega_1 T_{90^\circ})$ (reduced χ^2 of 42.1). This proves that the RF field inhomogeneity is not constant along a pulse sequence. It is not sufficient to conclude on the independence of two successive pulses but this would simply lead to an overestimation of the RF field amplitude inhomogeneity since the distribution obtained by scheme 1A is broader than that of scheme 1B. Anyway this result clearly indicates that the RF field inhomogeneity should be determined by adapting the sequence with which the measurement is done, in particular when one wants to take it into account in further data analysis.

B. Heteronuclear Case

It seems particularly relevant to adopt the same approach for any heteronuclear measurement, since two different coils are usually involved. Indeed the effective inhomogeneity (that which influences the measurements) is expected and effectively observed (data not shown) to be different from the complete inhomogeneity of the heteronuclear coil (usually the outer coil in an inverse probehead). We have considered as an example of a reference experiment the self-relaxation rate measurement in the presence of an off-resonance RF irradiation with adiabatic rotations (*18, 19*). Since in that experiment the ^{15}N magnetization is adiabatically rotated from the static magnetic field direction toward the tilted effective field at the beginning of the spin-lock and back at its end, the relative

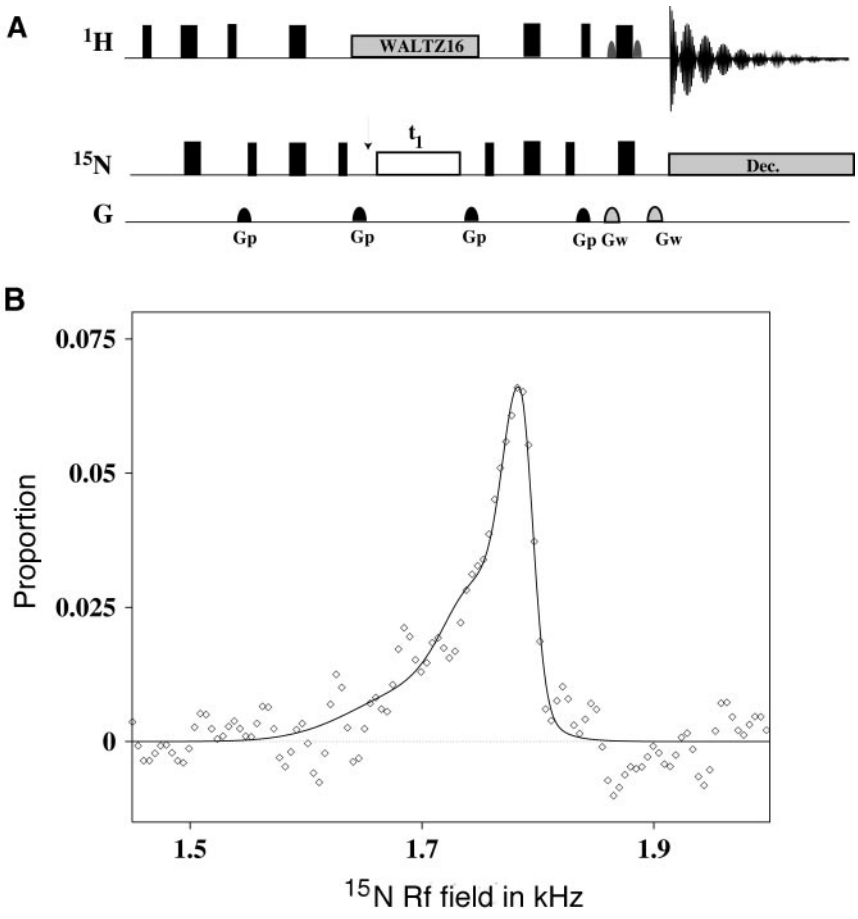

FIG. 3. (A) Pulse sequence allowing the determination of the RF field inhomogeneity relevant for an off-resonance heteronuclear self-relaxation rate measurement using adiabatic rotations. Narrow and large filled boxes represents 90° and 180° hard pulses, respectively. The encoding gradient pulses of the WATERGATE sequence are denoted Gw. The phase cycling is the same as that used for longitudinal self-relaxation measurement. The arrow indicates the position where off-resonance RF irradiation can be added to follow the variation of the RF power after a strong irradiation. (B) Distribution of ^{15}N RF field inhomogeneity observed in a Bruker *z* gradient broadband inverse probehead. The solid line superimposed is a visually adjusted analytical representation of the experimental observation. Its equation is for $\omega_1 < 1785$ Hz, $4.210^{-4}e^{-(\omega_1-1785/21)2} + 1.810^{-4}e^{-(\omega_1-1750/40)2} + 0.810^{-4}e^{-(\omega_1-1700/80)2}$ and for $\omega_1 > 1785$ Hz the first Gaussian is replaced by $4.210^{-4}e^{-(\omega_1-1785/15)2}$. This spectrum has been acquired at 310 K on a ^{15}N-enriched sample of Toxin α in water on a Bruker DRX500 spectrometer. The F_1 spectral width is 2.5 kHz, 200 FIDs have been acquired, the processed spectrum contains 512 real points in that dimension.

phase of the RF irradiation experienced by each voxel has no influence on the signal intensity, and the only relevant inhomogeneity is the amplitude one. The pulse sequence used for its determination is displayed in Fig. 3A. It was designed by simply replacing the spin-lock irradiation of fixed duration in the $R_{1\rho}^{\text{off}}$ pulse sequence (*18*) by a nutation period followed by a purging B_0 gradient pulse. Figure 3B shows a result obtained on a Bruker *z* gradient inverse broadband probehead with a ^{15}N-enriched Toxin α sample in water (*20*). The distribution of B_1 field is still asymmetrical. We define the ^{15}N nominal field, $B_{1\,\text{nom.}} = \omega_{1\,\text{nom.}}/\gamma$, as the RF field for which the probability $\mathcal{P}(\omega_1)$ is maximum. In order to have an analytical description of the experimental B_1 field distribution which can be used to simulate, for instance, the effect of the inhomogeneity on the HOHAHA coherence transfer, we have noticed that the experimental distribution can appropriately be described by the sum of two Gaussians and two half-Gaussians. The two half-Gaussians are centered at $B_{1\,\text{nom.}}$. As an example, a fitted curve is superimposed on the data points in Fig. 3B. Finally if we replace in the pulse sequence the nutation followed by a purging gradient pulse by just the nutation, as done in the homonuclear case (Fig. 1), we still do not observe the same distribution curve as for protons (Fig. 2).

The sequence of Fig. 3A has appeared to us as a very fast and accurate method for determining the heteronuclear RF field amplitude whatever its value. Indeed for a 5 mM ^{15}N protein, the determination of $B_{1\,\text{nom.}}$ requires about 10 mn. Relative determinations by physical methods based on signal sent to the probe (oscilloscope, powermeter, etc.) are, of course, faster but do not take into account every mismatching condition which can appear on the excitation line, resulting from nonlinearities in the response of the probehead, the preamplifier, the ampli-

fier, or the coil and which can vary along the sequence. They can simply result from heating. The approach based on the sequence of Fig. 3A makes it possible to check the response of the spectrometer after long irradiation or strong decoupling by, for example, adding an irradiation period just before the nutation (Its position is indicated by the arrow on Fig. 3A. We will denote its strength as $B_{1\,\mathrm{irr}}$, while the nominal RF field measured by the nutation will be noted $B_{1\,\mathrm{nut}}$.). On all the Bruker systems we have tested (three DRX spectrometers, each with two 300-W *X* amplifiers and the following 5-mm probeheads: *z* gradient broadband inverse (BBI), one- or three-axis gradients $^{15}N/^{13}C/^{1}H$ inverse (TXI), and or three-axis gradients $^{15}N/BB/^{1}H$ inverse (TBI)), applying an irradiation at a power of 5 W during 500 ms induced no significant power drop at that power level but significant power drops, up to 20%, at high power (>100 W). Consequently the hard pulses following the irradiation period are no longer well calibrated. This results in sensitivity losses that vary with the duration of the irradiation period. When a series of experiments is recorded with various mixing times to evaluate the magnetization decay rate in the presence of RF irradiation, these sensitivity losses due to power drop will bias the results. The extent of the amplifier power losses depends on many parameters (tuning, matching and choice of the probehead, amplifier, duration and power of irradiation, recovery delay after the irradiation, recycling delay, etc.). It always increases with the power request after the irradiation period (increase of $B_{1\,\mathrm{nut}}$) and with the strength of the long irradiation (increase of $B_{1\,\mathrm{irr}}$). This effect does not simply result from heating. Indeed if the irradiation period of amplitude $B_{1\,\mathrm{irr}}$ is applied before the recovery delay, as suggested when performing measurements at constant average RF power delivery (*21*), the power loss on $B_{1\,\mathrm{nut}}$ is extremely reduced whatever the choice of the power level. Also, if two 300-W *X* amplifiers are used to produce the ^{15}N pulses, one for the long irradiation ($B_{1\,\mathrm{irr}}$) and the second for the hard pulses and the decoupling period, or if a 500-W amplifier is used with the same powers for the irradiations as those used with a 300-W amplifier, no power loss is observed. This set of results proves that the principal reason for the power loss resides in a droop of the amplifier, but since we have never observed it when the signal is directly sent to an oscilloscope, it should, at least partially, result from the detuning of the excitation line. This is confirmed as we observe that the choice of the probehead has a strong influence on the amplifier power loss. In our hands, among all the probeheads we have used, it was the inverse broadband with one-axis gradient which gave the best results. To illustrate these observations, we report in Table 1 the results of the RF field amplitude measurements $B_{1\,\mathrm{nut}}$ performed on a Bruker DRX600 spectrometer equipped with a three-axis gradients TBI probehead and using the broadband channel for the ^{15}N pulses. These measurements were carried out using the pulse sequence displayed in Fig. 3A, incorporating an off-resonance RF irradiation with adiabatic rotations prior to the nutation period (position denoted by the arrow).

TABLE 1

High Power (200 W) Effective ^{15}N Nominal RF Field Strengths Measured Using the Sequence 3A Modified to Include at the Position Indicated by an Arrow an Extra Off-Resonance Spin-Lock of Different Durations and Strengths

	Duration					
	10 ms		150 ms		400 ms	
$\gamma B_{1\,\mathrm{irr}}$	$\gamma B_{1\,\mathrm{nut}}$	%	$\gamma B_{1\,\mathrm{nut}}$	%	$\gamma B_{1\,\mathrm{nut}}$	%
0.88 kHz	9.021	0.00	8.980	0.03	8.953	0.07
2 kHz	9.171	0.00	8.980	0.53	8.586	4.92

Note. In the denoted $\gamma B_{1\,\mathrm{nut}}$ columns are reported the measured RF field amplitudes in kilohertz. In the % columns is reported the calculated sensitivity loss after the refocused INEPT block assuming (i) that pulses were calibrated according to the field strength observed in the 10-ms irradiation experiment, and (ii) that the delivered field strength remains constant during the 10-ms duration of the double INEPT sequence. The irradiation was applied with an offset Δ of 12 kHz, which is high when having a low θ angle (9.4° at 2.2 kHz and 4.2° at 0.88 kHz, respectively), but moderate when staying in the fine band of optimal tuning/matching of the probe. Measurements were carried out with a 5 mM sample of fully enriched Toxin α on a Bruker DRX600 spectrometer equipped with a triple-axis gradient TBI probehead and a BLAX-H 300 amplifier (maximal delivery power of 300 W) to irradiate the heteronucleus. The different nitrogen pulses were applied at powers of 200 W (hard pulses), 5.3 W (decoupling during the 0.34-s acquisition time), 9.9 W (2.2-kHz spin-lock), and 1.9 W (0.88-kHz spin-lock). The repetition time was fixed to 2 s which is a typical value used in experiments recorded to measure relaxation times. In the F_1 dimension the spectral width was equal to 10 kHz, 64 FIDs had been acquired, and the spectra had been processed on 512 real points. The FWMH was about 330 Hz; the precision of the nominal $\gamma B_{1\,\mathrm{nut}}$ field could be estimated to be less than 50 Hz (*25*).

Hard pulses were applied at a power of 200 W with a 300-W amplifier. This table also reports an estimation of the sensitivity losses (til about 5%) after the refocused INEPT transfer resulting from miscalibrated pulses. These estimations were computed assuming the amplifier does not recover during the 10-ms duration of the refocused INEPT.

IV. EFFECT OF THE RF FIELD INHOMOGENEITY ON THE HETERONUCLEAR SELF-RELAXATION RATE DETERMINATION

In the presence of off-resonance RF irradiation, following the magnetization decay in a series of recorded experiments with various mixing times gives the off-resonance self-relaxation rates $R_{1\rho}^{\mathrm{off}}$ of the one spin-order coherences (S_Z) aligned with the effective field [22]

$$R_{1\rho}^{\mathrm{off}} = \cos^2\theta R_1 + \sin^2\theta R_2 + \sin^2\theta J_{\mathrm{ex}}(\Omega), \qquad [10]$$

where J_{ex} is an eventual fast chemical exchange contribution. Considering a two-site jump model with populations p_a and p_b

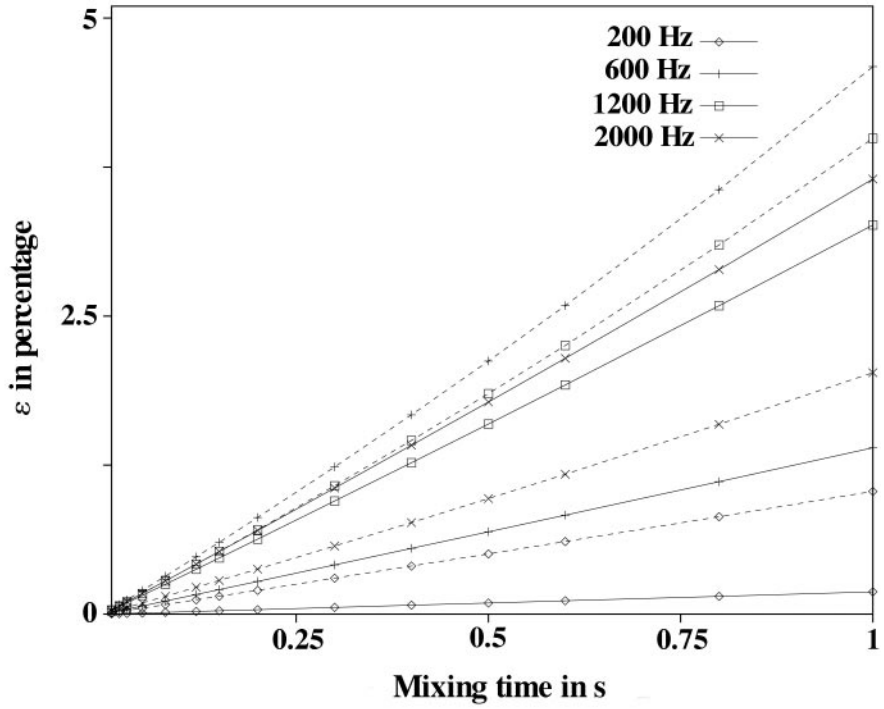

FIG. 4. Relative errors ϵ on the measured intensities resulting from RF field inhomogeneity. The system relaxes toward 0 in the absence of fast chemical exchange. Two experimentally determined RF field distributions are considered, one of $\gamma B_{1\,\mathrm{nom.}} = 862$ Hz (dashed lines) and the second of 1785 Hz (solid lines). Four different offsets (200, 600, 1200, and 2000 Hz) are considered. The longitudinal (R_1) and transverse (R_2) self-relaxation rates are taken equal to 2 and 5 Hz respectively.

and difference of resonance frequency $\delta\nu$, and denoting τ_e as the exchange correlation time, one has

$$J_{\mathrm{ex}}(\Omega) = p_a p_b \delta\nu^2 \frac{\tau_e}{1 + \Omega^2\tau_e^2}. \qquad [11]$$

Due to B_1 inhomogeneity, each voxel of the sample experiences a different RF field amplitude and thus a different angle θ (Eq. [7]). Because of Eq. [10], the relaxation rate varies from one voxel to the next as a function of inhomogeneity. For each voxel the decay is monoexponential, but as the system is nonlinear, the total magnetization decay is, a priori, no longer monoexponential. Since the function used to fit the experimental points (one exponential) does not correspond to the analytical solution, the extent of the bias induced by the RF field inhomogeneity on the relaxation rate depends on the number and values of the mixing times. However it is possible by numerical integration to compare the magnetization after relaxation during a mixing time τ_m in the presence of an inhomogeneous RF field to that in the presence of an homogeneous RF field. In this reference experiment the RF field amplitude is taken to be equal to the nominal one, $B_{1\,\mathrm{nom.}}$. We consider two schemes where either magnetization relaxes toward 0 (*23*) or toward its steady-state value which depends on θ. Using an experimentally observed RF field homogeneity (Fig. 3B and another acquired at a lower RF power), we compute the relative error ϵ

$$\epsilon = \frac{I_{\mathrm{inhom.}} - I_{\mathrm{hom.}}}{I_{\mathrm{hom.}}}, \qquad [12]$$

where $I_{\mathrm{inhom.}}$ is the intensity when RF field inhomogeneity is considered

$$I_{\mathrm{inhom.}} = I_0 \int_0^\infty \mathcal{P}(\omega_1)\left[\left(1 - \frac{I_\infty(\omega_1)}{I_0}\right)e^{-\tau_m R_{1\rho}^{\mathrm{off}}(\omega_1)} + \frac{I_\infty(\omega_1)}{I_0}\right]d\omega_1, \qquad [13]$$

while $I_{\mathrm{hom.}}$ represents magnetization in a purely homogeneous RF field of amplitude $B_{1\,\mathrm{nom.}}$, formally

$$I_{\mathrm{hom.}} = (I_0 - I_\infty(\omega_{1\,\mathrm{nom.}}))e^{-\tau_m R_{1\rho}^{\mathrm{off}}(\omega_{1\,\mathrm{nom.}})} + I_\infty(\omega_{1\,\mathrm{nom.}}), \qquad [14]$$

where $I_\infty(\omega_1)$ is the intensity at $\tau_m = \infty$ which depends on ω_1 at least through the angle θ (*24*).

In Fig. 4 the results computed considering different offsets Δ (i.e., different angles θ) in the off-resonance ^{15}N self-relaxation scheme (*18*) are displayed. First the relative error increases

with the mixing time, reaching values of 2 to 4%. Larger values are obtained, if we consider the scheme where the magnetization tends toward its steady-state value (data not shown). The scheme in which the magnetization decays toward zero enables a more precise determination of the relaxation rate by reducing the unknowns from 3 (I_0, $R_{1\rho}^{\text{off}}$, I_∞) to 2 (I_0, $R_{1\rho}^{\text{off}}$). In the present study, we show that this is strengthened by the fact that the long mixing time points are no longer required, i.e., those for which the error is at its largest. Second, due to angular dispersion, ϵ varies in opposite direction to the RF field strength $B_{1\,\text{nom}}$ and is maximal at a particular offset Δ.

When fast chemical exchange contributes to relaxation, the RF field inhomogeneity has two effects. First, as considered above, the direction of the effective field exhibits a certain distribution. Second, the effective field amplitude Ω (Eq. [8]) also varies all over the sample. Consequently, even if the spin-lock is applied on-resonance, the RF field inhomogeneity influences the magnetization decay through the chemical exchange contribution $J_{\text{ex}}(\Omega)$. The same comparison as above was carried out, indicating that the relative error ϵ is about twice as large as that found in the absence of chemical exchange. In that case, ϵ can reach values on the order of 5% whatever the used scheme.

V. CONCLUSIONS

According to the pulse sequence used, either the RF field amplitude distribution alone or the combined effect of RF field amplitude and phase inhomogeneities all over the sample influences the measurement. These distributions can experimentally be determined respectively by a nutation period followed by a purging gradient pulse and by a single nutation period. The RF field inhomogeneity induces biases on the heteronuclear transverse self-relaxation determination. The measured intensities can be erroneous by about 2%, when fast chemical exchange does not contribute to relaxation but can reach 5% if fast chemical exchange is present. To avoid this, we suggest using the experimental B_1 field distribution to calculate the magnetization decay and then to determine the transverse self-relaxation rate or the parameters of the fast chemical exchange. The flexibility of the method has allowed us not only to determine the biases induced by the RF field inhomogeneity on the measured intensities, but also to follow the RF power along the sequence. Therefore it has revealed possible power losses after RF irradiation which can induce an apparent decay of about 5% of the signal intensity. To avoid this artifact, it seems important to avoid working near the limit of maximal delivery power of the amplifier. To still maintain short ^{15}N hard pulses it is possible to resort either to very high power amplifiers ($>$500 W) or to share the X pulses and irradiations between two X amplifiers. These two results lead us to the conclusion that the error on relaxation rates cannot be deduced only from reproducibility measurements.

ACKNOWLEDGMENTS

The authors are indebted to Dr. Martial Piotto from Bruker Company for many fruitful discussions on the RF amplifiers and for providing us with a BLAX-500 amplifier and high power couplers. We acknowledge Dr. Frans A. A. Mulder for having sent us a preprint of Ref. (*19*).

REFERENCES

1. L. E. Kay, D. A. Torchia, and A. Bax, Backbone dynamics of proteins as studied by ^{15}N inverse detected heteronuclear NMR spectroscopy: application to Staphylococcal nuclease, *Biochemistry* **28,** 8972–8979 (1989).
2. J. W. Peng and G. Wagner, Mapping the spectral density functions using heteronuclear NMR relaxation measurements, *J. Magn. Reson.* **98,** 308–322 (1992).
3. G. Wagner, NMR relaxation and protein mobility, *Curr. Opin. Struct. Biol.* **3,** 748–754 (1993).
4. A. G. Palmer, III, J. Williams, and A. McDermott, Nuclear magnetic resonance studies of biopolymer dynamics, *J. Phys. Chem.* **100,** 13,293–13,310 (1996).
5. R. Brüschweiler, X. Liao, and P. Wright, Long-range motional restrictions in a multidomain Zinc-finger protein from anisotropic tumbling, *Science* **268,** 886–889 (1995).
6. N. Tjandra, S. E. Feller, R. W. Pastor, and A. Bax, A rotational diffusion anisotropy of human ubiquitin from ^{15}N NMR relaxation, *J. Am. Chem. Soc.* **117,** 12,562–12,566 (1995).
7. N. Tjandra, D. S. Garrett, A. M. Gronenborn, A. Bax, and G. M. Clore, Defining long range order in NMR structure determination from the dependence of heteronuclear relaxation times on rotational diffusion anisotropy, *Nat. Struct. Biol.* **4,** 443–449 (1997).
8. M. Akke, J. Liu, J. Cavanagh, H. B. Erickson, and A. G. Palmer III, Pervasive conformational fluctuations on microsecond time scale in a febronectin type III domain, *Nat. Struct. Biol.* **5,** 55–59 (1998).
9. L. K. Lee, M. Rance, W. J. Chazin, and A. G. Palmer III, Rotational diffusion anisotropy of proteins from simultaneous analysis of ^{15}N and $^{13}C_\alpha$ nuclear spin relaxation, *J. Biomol. NMR* **9,** 287–298 (1997).
10. T. E. Bull, Effect of rf field inhomogeneities on spin-echo measurements, *Rev. Sci. Instrum.* **45,** 232–242 (1974).
11. J. Murphy-Boesch, G. J. So, and T. L. James, Precision mapping of the B_1 field using the rotating-frame experiment, *J. Magn. Reson.* **73,** 293–303 (1987).
12. R. Tanaka, Y. Kida, K. Hasegawa, and H. Suematsu, B_1 maps of PFG probes, *in* "37th Experimental NMR Conference, March 17–22, 1996, Asilomar, California."
13. H. C. Torrey, Transient nutations in nuclear magnetic resonance, *Phys. Rev.* **76,** 1057–1068 (1949).
14. J. S. Leigh Jr., New technique for radio frequency magnetic field measurement, *Rev. Sci. Instrum.* **39,** 1594–1595 (1968).
15. A. Bax, "Two Dimensional Nuclear Magnetic Resonance in Liquids," Deft University Press, Reidel, Dortrecht (1982).
16. F. J. M. van de Ven, "Multidimensional NMR in liquids," VCH, New York (1995).
17. D. I. Hoult and R. E. Richards, The signal-to-noise ratio of nuclear magnetic resonance experiments, *J. Magn. Reson.* **24,** 71–85 (1976).

18. S. Zinn-Justin, P. Berthault, M. Guenneuges, and H. Desvaux, Off-resonance rf fields in heteronuclear NMR. Application to the study of slow motions, *J. Biomol. NMR* **10,** 363–372 (1997).

19. F. A. A. Mulder, R. A. de Graaf, R. Kaptein, and R. Boelens, An off-resonance rotating frame relaxation experiment for the investigation of macromolecular dynamics using adiabatic rotations, *J. Magn. Reson.* **131,** 351–357 (1998).

20. P. Drevet, C. Lemaire, S. Gasparini, S. Zinn-Justin, E. Lajeunesse, F. Ducancel, O. Trémeau, M. Courson, J.-C. Boulain, and A. Ménez, High level production and isotope labeling of snake neurotoxins, disulphide rich proteins, *Protein Expression Purif.* **10,** 293–300 (1997).

21. A. C. Wang and A. Bax, Minimizing the effects of radio-frequency heating in multidimensional NMR experiments, *J. Biomol. NMR* **3,** 715–720 (1993).

22. D. G. Davis, M. E. Perlman, and R. E. London, Direct measurements of the dissociation-rate constant for inhibitor-enzyme complexes via $T_{1\rho}$ and T_2 (CPMG) methods, *J. Magn. Reson. B* **104,** 266–275 (1994).

23. V. Sklenář, D. Torchia, and A. Bax, Measurement of Carbon-13 longitudinal relaxation using ^{1}H detection, *J. Magn. Reson.* **73,** 375–379 (1987).

24. M. Goldman, Formal theory of spin-lattice relaxation, *Adv. Magn. Opt. Reson.,* in press (1998).

25. G. H. Weiss, J. A. Ferretti, and J. A. Kiefer, A study of precision in the measurement of chemical shifts, *J. Magn. Reson.* **46,** 69–83 (1982).